

Stable Operating Region in a Harmonically Actively Mode-Locked Fiber Laser

Avi Zeitouny, Yuriy N. Parkhomenko, and Moshe Horowitz

Abstract—We theoretically study the recovery of a harmonically actively mode-locked soliton fiber laser from pulse dropout. In such lasers, a large number of pulses propagate simultaneously in the cavity. In order to obtain stable operation, pulses that are dropped due to changes in environmental conditions should recover, while other pulses that propagate in the cavity should remain stable. Soliton perturbation theory is used to find stability conditions for the noise in a time slot where a steady state pulse exists and in a time slot where a pulse is dropped. In the stable operating region of the laser, noise is stable in the presence of a pulse while noise becomes unstable in time slots where a pulse is dropped. Such a stability condition ensures that the laser can recover from accidental pulse dropout. A good agreement between the results of a reduced model and the results of a comprehensive numerical simulation was obtained. The results of this paper may enable to improve the stability of actively mode-locked fiber lasers.

Index Terms—Optical fiber lasers, perturbation methods.

I. INTRODUCTION

ACTIVELY mode-locked fiber lasers have been intensively studied, both theoretically and experimentally. Many of the theoretical studies are based on solving the equation known as the modified Ginzburg–Landau equation or the master equation of mode-locking [1]–[5]. This approach has enabled to study the noise of mode-locked lasers [6]–[9] by modeling the noise as a small perturbation added to the steady state pulse. Kärtner *et al.* [8] used such theory to analyze the noise in an actively mode-locked laser that generates solitary pulses. The nonlinear effect in such a laser shortens the pulse duration. Analysis of the stability of the noise shows that the minimum pulse duration is limited in such lasers due to the instability of the noise.

Numerical simulations enable to study the propagation of several pulses in the cavity, rather than a single pulse [10]. As the power in the cavity of an actively mode-locked fiber laser increases, the pulses evolve through four different operating regimes. In the first regime, the nonlinear effect is negligible and the pulse length is limited by the Kuizenga–Seigman limit [11]. As the power increases, the Kerr effect begins to affect the pulses, resulting in pulse shortening, but the pulse train is subject to a large amount of dropout. The stable operating regime is the third regime, with a very low dropout ratio. However, practical lasers that operate in this region are subject to pulse dropout due to changes in environmental conditions [12], [13]. In order to obtain stable operation, the laser should quickly recover from

accidental pulse dropout. When the power is further increased, a fourth operating regime is reached, in which pulse pairs are formed in some of the time slots.

In a practical harmonically mode-locked fiber laser, pulses may be dropped due to changes in environmental conditions. Such pulses should quickly recover in order to avoid supermode competition that may lead to system errors. In this work we study the conditions required for a harmonically actively mode-locked fiber laser to be able to recover from pulse dropout. Our analysis indicates that stable pulses can propagate inside the laser cavity while other pulses that are dropped can be regenerated. This result extends, for a fiber laser, a previous result that indicated that when stable pulses are generated, the noise does not grow in a time slot where a pulse is missing and therefore such a laser cannot recover from pulse dropout [8]. We study the stability of the noise accompanying a pulse that propagates in the cavity, and compare the results to the stability of noise that remains where a pulse is dropped. Soliton perturbation theory may be used to analyze the stability of the noise [8], [14]. When only a single pulse propagates inside the laser cavity, no dropout of pulses may occur. Therefore, previous analysis on noise stability in actively mode-locked lasers showed that the noise behavior was the same in a time slot where a pulse exists and in a time slot where a pulse is dropped [8]. This result was obtained because mathematical terms that represent the dependence of the noise on the pulse could be neglected, to first order, when only a single pulse propagated inside the cavity. Our stability analysis indicates that in the optimal operating region of the laser, noise in a time slot where a pulse is dropped is unstable while the noise in a time slot where a pulse propagates is stable. We found that the noise in a time slot where a pulse propagates is stable since some of the noise is coupled into solitary modes by the modulator and the filter. The noise coupled to solitary modes is stabilized due to solitonic propagation of pulses in the cavity that tends to maintain the pulse shape against perturbations. The different behavior of the noise due to the existence of a pulse is essential to ensure a practical operation of fiber lasers. The laser can recover from pulse dropout in the optimal operating region, while the noise in the pulses remains very weak.

The manuscript is divided into four main sections. In Section II, we give the equation for analyzing the dynamics of the continuum. In Section III, we derive the conditions for the optimal operating region of the laser where the laser can recover from pulse dropout. In Section IV, we give numerical examples for the calculation of the boundaries of the stable operating region of the laser. In Section V, we compare the results of the reduced model to the results of a comprehensive numerical simulation.

Manuscript received April 18, 2005; revised July 14, 2005.

The authors are with the Technion—Israel Institute of Technology, Haifa 32000, Israel (e-mail: avize@tx.technion.ac.il).

Digital Object Identifier 10.1109/JQE.2005.857054

II. MATHEMATICAL MODEL FOR CALCULATING THE CONTINUUM

In this section, we derive the mathematical framework used in our manuscript for analyzing actively mode-locked fiber lasers. The analysis given in this section shortly summarizes the results given in previous work [6]–[8]. We start our analysis using the master equation of mode-locking [2]

$$T_R \frac{\partial A(T, t)}{\partial T} = i \frac{D}{2} \frac{\partial^2 A(T, t)}{\partial t^2} - i \delta |A(T, t)|^2 A(T, t) + \left\{ \Delta G - l + \frac{F}{\Omega_F^2} \frac{\partial^2}{\partial t^2} - \frac{M}{2} [1 - \cos(\omega_M t)] \right\} \times A(T, t) + T_R n(T, t) \quad (1)$$

where T is a slow time variable on the scale of the cavity round-trip time T_R , t is a fast time variable on the order of the pulse duration, D is the intracavity dispersion per round-trip, δ is the Kerr coefficient per round-trip, ΔG is the saturated gain, l is the linear loss, M is the modulation depth, F is the filter transmission at its central wavelength, Ω_F is the filter bandwidth, ω_M is the modulation frequency, $A(T, t)$ is the complex envelope of the pulse, and $n(T, t)$ is an additive noise source resulting from the spontaneous emission of the amplifier. We assume that the amplifier response time is significantly longer than the time scale used in our stability analysis and therefore the amplifier dynamics can be neglected. The filter in the cavity is formed by the amplifier bandwidth or by an additional filter added to the cavity. Assuming that the linear loss, l , is significantly larger than the loss that depends on the pulse parameters, we neglect the change in the amplifier's filtering effect as a function of the gain ΔG , as assumed in [14].

We assume that the modulator and the filter cause only a small change in the pulse that propagates through the fiber and therefore the pulse shape remains nearly secant-hyperbolic [7], [8]. Hence, the solution for the master equation can be written as

$$A(T, t) = [a(x) + \Delta a(T, x)] \exp\left(-i \frac{\delta A_0^2 T}{2 T_R}\right) \quad (2)$$

where

$$a(x) = A_0 \operatorname{sech}(x), \quad x = \frac{t}{\tau} \quad (3)$$

is the unperturbed solution, τ is the length of the unperturbed soliton, and x relates to the short time scale t as above. We assume that the change in the pulse shape due to the amplifier, the filter, and the modulator is small and therefore the function $\Delta a(T, x)$ can be treated as a small perturbation. We use a vectorial notation for the perturbation, as used in [7], [8], $\Delta \mathbf{a} = \begin{pmatrix} \Delta a(T, x) \\ \Delta a^*(T, x) \end{pmatrix}$. Similar notation is used for the variables \mathbf{n} and \mathbf{a} . The dynamic behavior of the perturbation is obtained by substituting (2) into (1) and expanding the result up to first order in Δa

$$T_R \frac{\partial \Delta \mathbf{a}}{\partial T} = -i \Phi \mathbf{L} \Delta \mathbf{a} + \mathbf{R}(\mathbf{a} + \Delta \mathbf{a}) + T_R \mathbf{n}(T, t) \quad (4)$$

where

$$\mathbf{L} = \begin{pmatrix} -\left(1 - \frac{\partial^2}{\partial x^2} - 4 \operatorname{sech}^2 x\right) & 2 \operatorname{sech}^2 x \\ -2 \operatorname{sech}^2 x & \left(1 - \frac{\partial^2}{\partial x^2} - 4 \operatorname{sech}^2 x\right) \end{pmatrix} \quad (5a)$$

$$\mathbf{R} = \Delta G - l + \frac{F}{\Omega_F^2 \tau^2} \frac{\partial^2}{\partial x^2} - \frac{M}{2} [1 - \cos(\omega_M \tau x)] \quad (5b)$$

$$\Phi = \frac{\delta A_0^2}{2} = -\frac{D}{2\tau^2} > 0. \quad (5c)$$

In deriving (4), it is assumed that Δa may be considered as a perturbation to the soliton. However, the term $R\Delta a$ in (4) is not neglected, since its magnitude depends on the particular function Δa . Therefore, the term $R\Delta a$ may be on the same order as the term Δa . In deriving (4) we used the relation $|D|/(2\tau^2) = \delta A_0^2/2$, obtained from the zero order solution.

Equation (4) gives the evolution of the perturbation Δa on the time T . The operator \mathbf{L} gives the effect of the propagation through the fiber, due to dispersion and Kerr effect. The operator \mathbf{R} gives the effect of the amplifier, the filter, and the modulator. We will expand the perturbation, Δa , as a linear sum of the eigenstates of the operator \mathbf{L} . Reference [7] gives the eigenfunctions of the operator \mathbf{L} , and defines an inner product under which the operator \mathbf{L} is a self-adjoint operator. The perturbation Δa can be expanded as a linear sum of the eigenstates of the operator \mathbf{L} [7]

$$\Delta \mathbf{a} = \Delta W(T) \mathbf{f}_w + \Delta t(T) \mathbf{f}_t + \Delta \theta(T) \mathbf{f}_\theta + \Delta p(T) \mathbf{f}_p + \mathbf{a}_c \quad (6)$$

where \mathbf{f}_w , \mathbf{f}_θ , \mathbf{f}_p , and \mathbf{f}_t are the discrete states of the operator \mathbf{L} that give the changes in the soliton energy, phase, carrier frequency, and timing, respectively [6], [8]

$$\mathbf{f}_\theta(x) = ia(x) \begin{pmatrix} 1 \\ -1 \end{pmatrix} \quad (7a)$$

$$\mathbf{f}_t(x) = \frac{1}{\tau} \tanh(x) a(x) \begin{pmatrix} 1 \\ 1 \end{pmatrix} \quad (7b)$$

$$\mathbf{f}_w(x) = \frac{1}{W} [1 - x \tanh(x)] a(x) \begin{pmatrix} 1 \\ 1 \end{pmatrix} \quad (7c)$$

$$\mathbf{f}_p(x) = ix\tau a(x) \begin{pmatrix} 1 \\ -1 \end{pmatrix} \quad (7d)$$

where $W = 2\tau A_0^2$ is the energy of the soliton. The continuum may be expanded using the continuous spectrum of the operator \mathbf{L} , $\boldsymbol{\psi}_k(x)$ and $\bar{\boldsymbol{\psi}}_k(x)$ [7]

$$\mathbf{a}_c = \int_{-\infty}^{\infty} [g(T, k) \boldsymbol{\psi}_k + \bar{g}(T, k) \bar{\boldsymbol{\psi}}_k] dk \quad (8)$$

where

$$\boldsymbol{\psi}_k(x) = \frac{e^{ikx}}{(k+i)^2} \begin{pmatrix} \operatorname{sech}^2 x \\ (k+i \tanh x)^2 \end{pmatrix} \quad (9a)$$

$$\bar{\boldsymbol{\psi}}_k(x) = \frac{e^{ikx}}{(k+i)^2} \begin{pmatrix} (k+i \tanh x)^2 \\ \operatorname{sech}^2 x \end{pmatrix}. \quad (9b)$$

Instability of the laser pulses can occur due to the instability of the discrete states of the soliton or due to the instability of the continuum. The stability of the discrete states of the soliton was studied in [6], [14], and [15]. The jitter and the frequency of the

soliton are stabilized due to the modulator and filter, respectively [2]. The stability condition for the pulse energy is given by [14]

$$\frac{\pi^2}{48} M \omega_M^2 \tau^2 - \frac{1}{3} \frac{F}{\Omega_F^2 \tau^2} < 0. \quad (10)$$

As the power in the laser is increased, the pulses become shorter, and the second term in (10), that represents the effect of the filter, becomes larger. A stable operation is obtained when the filter effect becomes stronger than the effect of the modulator. Therefore, when the power inside the laser is increased above a certain level the pulses become short enough and the pulse energy becomes stable. Assuming that the laser power is above the threshold needed for the stability of the discrete states of the soliton, we will focus on the stability of the continuum and find the maximum power of the stable operating region of the laser.

Using (8), it can be shown that

$$\begin{aligned} \bar{g}(T, k) &= g^*(T, -k) \\ a_c(T, x) &= \tilde{g}(T, x) \operatorname{sech}^2(x) - \frac{d^2}{dx^2} \tilde{g}^*(T, x) \\ &\quad + 2 \tanh(x) \frac{d}{dx} \tilde{g}^*(T, x) - \tanh^2(x) \tilde{g}^*(T, x) \end{aligned} \quad (11)$$

where

$$\tilde{g}(T, x) = \int_{-\infty}^{\infty} \frac{e^{ikx}}{(k+i)^2} g(T, k) dk. \quad (13)$$

Thus, the stability of the continuum is determined by the stability of the function $g(T, k)$.

We find the equation of motion for $g(T, k)$ by projecting (4) onto the continuous eigenstates of the operator \mathbf{L} $\phi_k(x)$, and $\bar{\phi}_k(x)$ [7]

$$\phi_k(x) = \frac{e^{-ikx}}{(k+i)^2} \begin{pmatrix} (k-i \tanh x)^2 \\ \operatorname{sech}^2 x \end{pmatrix} \quad (14a)$$

$$\bar{\phi}_k(x) = \frac{e^{-ikx}}{(k+i)^2} \begin{pmatrix} \operatorname{sech}^2 x \\ (k-i \tanh x)^2 \end{pmatrix} \quad (14b)$$

Using (6) and (8)

$$\begin{aligned} T_R \frac{\partial g(T, k)}{\partial T} &= [\Delta G - l - i\Phi(k^2 + 1)]g(T, k) \\ &\quad + \frac{M}{4} [2g(T, k) - g(k + \omega_M \tau) - g(k - \omega_M \tau)] \\ &\quad - \frac{M}{2} I [f_M(k, k', \omega_M \tau)] \\ &\quad - \frac{M}{2} \bar{I} [\bar{f}_M(k, k', \omega_M \tau)] - \frac{F}{\Omega_F^2 \tau^2} k^2 g(T, k) \\ &\quad - \frac{F}{\Omega_F^2 \tau^2} I [f_F(k, k')] - \frac{F}{\Omega_F^2 \tau^2} \bar{I} [\bar{f}_F(k, k')] \\ &\quad - \frac{1}{2\pi a_k^2} \langle \bar{\phi}_k | \mathbf{R}(\Delta W \mathbf{f}_w + \Delta \theta \mathbf{f}_\theta + \Delta p \mathbf{f}_p + \Delta t \mathbf{f}_t) \rangle \\ &\quad - \frac{1}{2\pi a_k^2} \langle \bar{\phi}_k | \mathbf{R} \mathbf{a} \rangle - \frac{T_R}{2\pi a_k^2} \langle \bar{\phi}_k | \mathbf{n}(T, t) \rangle \end{aligned} \quad (15)$$

where

$$f_F(k, k') = \frac{1}{4} \frac{(k' - k)(k' + k)^2 (2 + k'^2 + k^2)}{(k' + i)^2 (k - i)^2} \operatorname{csch} \left[\frac{\pi}{2} (k' - k) \right] \quad (16a)$$

$$\begin{aligned} f_M(k, k', \omega_M \tau) &= \frac{1}{4} \frac{\omega_M \tau}{(k' + i)^2 (k - i)^2} \\ &\quad \cdot \left((2 + k'^2 + k^2) \left\{ \operatorname{csch} \left[\frac{\pi}{2} (k' - k + \omega_M \tau) \right] \right. \right. \\ &\quad \left. \left. - \operatorname{csch} \left[\frac{\pi}{2} (k' - k - \omega_M \tau) \right] \right\} + \omega_M \tau (k' - k) \right. \\ &\quad \left. \times \left\{ \operatorname{csch} \left[\frac{\pi}{2} (k' - k + \omega_M \tau) \right] \right. \right. \\ &\quad \left. \left. + \operatorname{csch} \left[\frac{\pi}{2} (k' - k - \omega_M \tau) \right] \right\} \right) \end{aligned} \quad (16b)$$

$$\begin{aligned} \bar{f}_F(k, k') &= -\frac{1}{4} \frac{(k' - k)^2 (k' + k)(2 + k'^2 + k^2)}{(k' + i)^2 (k - i)^2} \operatorname{csch} \left[\frac{\pi}{2} (k' - k) \right] \\ \bar{f}_M(k, k', \omega_M \tau) &= -\frac{1}{4} \frac{\omega_M \tau}{(k' + i)^2 (k - i)^2} \\ &\quad \cdot \left((k'^2 - k^2) \left\{ \operatorname{csch} \left[\frac{\pi}{2} (k' - k + \omega_M \tau) \right] \right. \right. \\ &\quad \left. \left. - \operatorname{csch} \left[\frac{\pi}{2} (k' - k - \omega_M \tau) \right] \right\} \right. \\ &\quad \left. + \omega_M \tau (k' + k) \left\{ \operatorname{csch} \left[\frac{\pi}{2} (k' - k + \omega_M \tau) \right] \right. \right. \\ &\quad \left. \left. + \operatorname{csch} \left[\frac{\pi}{2} (k' - k - \omega_M \tau) \right] \right\} \right) \end{aligned} \quad (16c)$$

and

$$\begin{aligned} I[f(k)] &= \int_{-\infty}^{\infty} f(k, k') g(k') dk' \\ \bar{I}[f(k)] &= \int_{-\infty}^{\infty} f(k, k') \bar{g}(k') dk' \end{aligned}$$

Each of the terms in (15) can be intuitively understood. The term $(\Delta G - l)g(T, k)$ represents the linear gain and loss experienced by the continuum. The term $-i\Phi(k^2 + 1)g(T, k)$ originates in the operator $-i\Phi \mathbf{L} \mathbf{a}_c$, and thus represents the effect of propagation through the fiber on the continuum. The modulator and the filter couple between different continuum modes. The terms $(M/4)2g(k)$ and $M/4[-g(k + \omega_M \tau) - g(k - \omega_M \tau)]$ represent the coupling of the continuum modes ψ_k and $\psi_{k \pm \omega_M \tau}$ into a mode $\bar{\phi}_k$, respectively, due to the modulator. The next two terms represent coupling by the modulator of continuum modes with a spectral component *around* k to the continuum modes with a spectral components $k \pm \omega_M \tau$. Since the functions that span the continuum, $\psi(k)$ and $\bar{\psi}(k)$, are not sinusoidal functions, the action of the modulator is not given by two delta functions at $k \pm \omega_M \tau$. The next three terms, with the coefficient $F/\Omega_F^2 \tau^2$, represent the action of the filter. The first term gives the effect of the spectral response of the filter on the continuum modes. The contribution of this term increases as k increases. The other two terms couple between the mode with a

spectral component k to other continuum components. The contribution of these terms increases as $k - k'$ increases; however, a plot of the function, $f_F(k, k')$, indicates that it reaches a constant value when the spectral frequency difference $k - k'$ becomes large enough. The last three terms in the equation correspond to nonhomogeneous terms. The first term describes the contribution of the solitonic noise to the continuum due to the propagation through the modulator, the amplifier, and the filter, that are presented by the operator \mathbf{R} . The term $-\langle \bar{\phi}_k | \mathbf{R} \mathbf{a} \rangle / 2\pi a_k^2$ represents the part of the perturbed soliton that is coupled into the continuum due to the modulator and the filter, and the term $-T_R \langle \bar{\phi}_k | \mathbf{n}(T, t) \rangle / 2\pi a_k^2$ represents the part of the additive noise that is coupled into the continuum.

III. STABILITY ANALYSIS OF THE CONTINUUM

In this section we find the stability condition for the continuum. Equation (15) can be further simplified using the assumption that the pulse duration is significantly smaller than the repetition time of the modulation frequency, i.e $\omega_M \tau < 1$, and therefore we neglect terms on the order of $\omega_M^4 \tau^4$ or higher and obtain:

$$T_R \frac{\partial g(T, k)}{\partial T} = (\hat{C} + \hat{H} + \hat{Q}) \cdot g(T, k) - \frac{1}{2\pi a_k^2} \langle \bar{\phi}_k | \mathbf{R} \mathbf{a} \rangle - \frac{T_R}{2\pi a_k^2} \langle \bar{\phi}_k | \mathbf{n}(T, t) \rangle - \frac{1}{2\pi a_k^2} \langle \bar{\phi}_k | \mathbf{R} (\Delta W \mathbf{f}_w + \Delta \theta \mathbf{f}_\theta + \Delta p \mathbf{f}_p + \Delta t \mathbf{f}_t) \rangle \quad (17)$$

where

$$\hat{C} g(T, k) = (\Delta G - l - i\Phi) g(T, k) \quad (18a)$$

$$\hat{H} g(T, k) = \left[\frac{M}{4} \omega_M^2 \tau^2 \frac{\partial^2}{\partial k^2} - \left(i\Phi + \frac{F}{\Omega_F^2 \tau^2} \right) k^2 \right] g(T, k) \quad (18b)$$

$$\hat{Q} g(T, k) = -\frac{F}{\Omega_F^2 \tau^2} I [f_F(k, k')] - \frac{M}{2} I [f_M(k, k', \omega_M \tau)] - \frac{F}{\Omega_F^2 \tau^2} \bar{I} [\bar{f}_F(k, k')] - \frac{M}{2} \bar{I} [\bar{f}_M(k, k', \omega_M \tau)] \quad (18c)$$

In [8], the stability of the continuum around the pulse was studied. However, in the analysis given in [8], the operator Q was neglected and therefore the stability condition obtained was the same for noise that propagates in a time slot where a pulse exists and in a time slot where a pulse is dropped. Using straightforward complex analysis, we approximated the integrals in the operator \hat{Q} and showed that the terms in the operator \hat{Q} , originating from the modulator, are on the order of $M\omega_M^2 \tau^2$. Similarly, we showed that the terms in the operator \hat{Q} , originating from the filter, are on the order of $F/\Omega_F^2 \tau^2$. Therefore, the effect of the operator \hat{Q} on the continuum is on the same order as the effect of the operator \hat{H} . In the next two sections, we will show that since in highly harmonically fiber lasers the operator \hat{Q} cannot be neglected, the stability condition for the noise that propagates in a time slot where a pulse exists is different from the stability condition for the noise in a time slot where a pulse is dropped. The difference in the stability conditions enables the

laser to generate stable solitary pulses and still be able to recover from pulse dropouts.

As explained in Section II, the stability of the continuum is determined by the stability of the function $g(T, k)$. The time dependent behavior of the continuum function $g(T, k)$ is given by (17). In order to find the stability condition for $g(T, k)$ we first solve the eigenvalue problem

$$(\hat{C} + \hat{H} + \hat{Q}) y_n(k) = \lambda_n y_n(k). \quad (19)$$

Then we can write $g(T, k)$ as a linear sum of the eigenfunctions $y_n(k)$

$$g(T, k) = \sum_n c_n(T) y_n(k). \quad (20)$$

Using (17), (19), and (20) we obtain

$$T_R \frac{\partial \Delta c_n(T)}{\partial T} = \lambda_n c_n(T) - \frac{1}{2\pi a_k^2} \langle y_n^\dagger(k) | \langle \bar{\phi}_k | \mathbf{R} \mathbf{a} \rangle \rangle - \frac{T_R}{2\pi a_k^2} \langle y_n^\dagger(k) | \langle \bar{\phi}_k | \mathbf{n}(T, t) \rangle \rangle - \frac{1}{2\pi a_k^2} \langle y_n^\dagger(k) | \langle \bar{\phi}_k | \mathbf{R} (\Delta W \mathbf{f}_w + \Delta \theta \mathbf{f}_\theta + \Delta p \mathbf{f}_p + \Delta t \mathbf{f}_t) \rangle \rangle \quad (21)$$

where $y_n^\dagger(k)$ is the adjoint function of $y_n(k)$.

Equation (21) is a stochastic linear first order differential equation. The equation may be divided into a homogenous part and into an inhomogeneous part. The stability of the homogenous part approximately gives the stability of (21). The inhomogeneous part may be divided into a stochastic term due to the amplifier noise and into a non stochastic term caused due to changes of the soliton in a round-trip. Since (21) is a first order differential equation the inhomogeneous term may cause a large increase in the solution close to the boundary of the stable region [16]. The stochastic part of the equation may also slightly change the boundary of the stable operating region, calculated from the homogenous part of the equation [17]. However, by comparing the reduced model with the results of a numerical simulation, as described in the next section, it can be shown that the magnitude of the inhomogeneous term is very small and it only slightly affects the stability of the equation. Moreover, the increase in the continuum intensity is obtained only very close to the boundary of the stable operating region. Therefore, we will determine the stability of the solution only according to the homogenous part of the equation.

The solution of the homogeneous part of (21) is

$$\Delta c_n(T) = \Delta c_n(0) \exp \left(\lambda_n \frac{T}{T_R} \right). \quad (22)$$

Therefore, the stability of the perturbation, $g(T, k)$, can be determined by the least stable eigenstate, i.e the eigenstate $y_n(k)$ with the eigenvalue that has the largest real part. Therefore, the stability condition is given by

$$\Lambda = \max_n \{ \text{Re} \{ \lambda_n \} \} < 0. \quad (23)$$

In order to find the eigenvalues of the operator $\hat{C} + \hat{H} + \hat{Q}$ we will first find the eigenvalues of the operator $\hat{C} + \hat{H}$ and

use the variational approach to add the important effect of the operator \hat{Q} . Since the operator \hat{C} is constant, the eigenfunctions of the operator $\hat{C} + \hat{H}$ will be determined by the eigenfunctions of the operator \hat{H} . The eigenvalue of the operator \hat{C} is equal to $\Delta G - l - i\Phi$. The operator \hat{H} corresponds to a harmonic oscillator with eigenvalues given by [18]

$$E_n^o = -2 \left[\frac{M}{4} \omega_M^2 \tau^2 \left(\frac{F}{\Omega_F^2 \tau^2} + i\phi \right) \right]^{\frac{1}{2}} \left(n + \frac{1}{2} \right) \quad (24)$$

and eigenstates

$$\varphi_n^o = N_n H_n \left(\frac{k}{\tau_k} \right) \exp \left(-\frac{k^2}{2\tau_k^2} \right) \quad (25)$$

where

$$\frac{1}{\tau_k} = \left[\frac{i\Phi + \frac{F}{\Omega_F^2 \tau^2}}{\frac{M}{4} \omega_M^2 \tau^2} \right]^{\frac{1}{2}}. \quad (26)$$

H_n are the Hermite polynomials, and N_n are normalization coefficients defined by biorthogonality of the operator, as described below. The operator \hat{H} is not hermitian and therefore it requires a careful consideration [19]. Under the definition of an inner product between two functions u and v

$$\langle u|v \rangle = \int_{-\infty}^{\infty} u^* v dx \quad (27)$$

the eigenstates of the adjoint operator $\tilde{\varphi}_n^o$ are the complex conjugates of the eigenstates φ_n^o . The coefficients \tilde{N}_n of the adjoint functions $\tilde{\varphi}_n^o$ are determined by the normalization requirement $\langle \tilde{\varphi}_n | \tilde{\varphi}_n \rangle = 1$. The normalization of the eigenmodes $\tilde{\varphi}_n^o$ combined with the biorthogonality requirement between the functions $\tilde{\varphi}_n^o$ and φ_n^o , requires that the normalization coefficients \tilde{N}_n will be different from the coefficients N_n . Using the above described normalization we obtain $\langle \tilde{\varphi}_p^o | \varphi_n^o \rangle = \delta_{pn}$; however, $|\tilde{\varphi}_p^o \rangle \langle \tilde{\varphi}_n^o|$ and $|\varphi_p^o \rangle \langle \varphi_n^o|$ are not diagonal [19].

In order to solve the eigenvalue of the complete operator, $\hat{C} + \hat{H} + \hat{Q}$, we use a variational approach [20], [21]. This method was successfully employed in numerous applications such as atomic and molecular physics, nuclear physics, and more [21]. The method is used to find the eigenvalues of a system when a direct calculation of the exact eigenstates cannot be performed. We define the functional of the state function b_n as $\langle E \rangle = \langle b_n^\dagger | \hat{C} + \hat{H} + \hat{Q} | b_n \rangle$, where b_n^\dagger is the adjoint state function of the function b_n . When b_n is an eigenfunction of the operator $\hat{C} + \hat{H} + \hat{Q}$, $\langle E \rangle$ is the eigenvalue E_n of the operator $\hat{C} + \hat{H} + \hat{Q}$ that corresponds to the eigenfunction b_n . Moreover, the function $\langle E \rangle$ is stationary in the neighborhood of the discrete eigenvalues of the operator $\hat{C} + \hat{H} + \hat{Q}$ [20]. Therefore, the calculation of the expectation value $\langle E \rangle$ from an approximate eigenstate of the operator, will often give a good approximation to the eigenvalue of the operator even when the approximate eigenstate of the operator is quite different from the accurate eigenstate. We choose to approximate the eigenstates of the operator $\hat{C} + \hat{H} + \hat{Q}$ as

the eigenstates of the operator $\hat{C} + \hat{H}$. Therefore, the eigenvalue, λ_n , of the operator $\hat{C} + \hat{H} + \hat{Q}$ can be approximated by $\Delta G + l + E_n^o + E_n^1$, where

$$E_n^1 = \langle \tilde{\varphi}_n^o | \hat{Q} | \varphi_n^o \rangle \quad (28)$$

and the stability condition is given by

$$\Lambda = \Delta G - l + \max_n \{ \text{Re} \{ E_n^o + E_n^1 \} \} < 0. \quad (29)$$

We have carefully checked the validity of the use of the variational approach in our laser using a comprehensive numerical simulation, as described in Section V. We obtained a good quantitative agreement between the results of the numerical simulation and the results obtained using the variational approach.

When the effect of the operator \hat{Q} on the continuum is neglected, as performed in [8], the stability condition is given by

$$\begin{aligned} \Lambda &= \Delta G - l + \text{Re} \{ E_o^o \} \\ &= \Delta G - l - \text{Re} \left\{ \left[\frac{M}{4} \omega_M^2 \tau^2 \left(\frac{F}{\Omega_F^2 \tau^2} + i\phi \right) \right]^{\frac{1}{2}} \right\} < 0 \end{aligned} \quad (30)$$

since $\max_n \{ \text{Re} \{ E_n^o \} \} = \text{Re} \{ E_o^o \}$. The result obtained is identical to the stability condition of the noise in a time slot where a pulse is absent [14]. However, in order to obtain stable operation of the laser, there should be an operating region where the noise in a time slot where a pulse exists is stable, while the noise in a time slot where a pulse is dropped is unstable. Therefore, in order to ensure optimal operation, both (29) and the condition

$$\Lambda = \Delta G - l + \text{Re} \{ E_o^o \} > 0 \quad (31)$$

should be met.

IV. NUMERICAL EXAMPLES

In this section, we give a numerical example for calculating the conditions required in order for the laser to be able to recover from pulse dropout. The stability of the noise in a time slot where a pulse propagates was calculated according to (29). The stability of the noise in a time slot where a pulse is missing was calculated using (31). In our calculations we assumed a loss per round-trip $l = 0.1$, modulation depth $M = 1$, negligible insertion loss of the filter, $F = 1$, nonlinear coefficient $\delta = 2.1 \cdot 0.05 = 0.105 \text{ W}^{-1}$, a cavity length of 50 m, and a filter bandwidth of 13.5 nm. The wide bandwidth of the filter used in the model as well as in experiments [22] enables to stabilize the pulses while not significantly limiting the pulse duration.

Fig. 1 shows the results of the stability analysis for a laser with a dispersion coefficient of 8 ps/(nm · km), a modulation frequency of 2 GHz, and a length of 50 m. The average power of the laser was calculated using the relation $P = W\omega_M/2\pi$, where $W = 2D/\tau\delta$ is the pulse energy. In order to find the incremental gain, ΔG , we used the equilibrium condition for the pulse energy [14]

$$\Delta G - l = \frac{\pi^2}{48} M \omega_M^2 \tau^2 + \frac{1}{3} \frac{F}{\Omega_F^2 \tau^2}. \quad (32)$$

The solid and the dashed lines in Fig. 1 give the results of (31) and (29), respectively. We also plotted the stability condition for

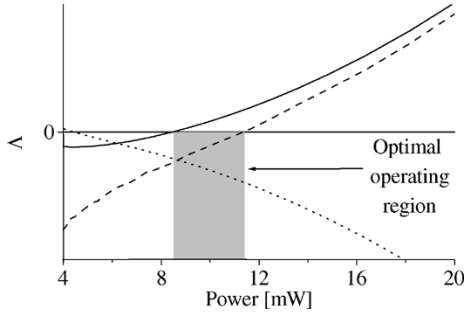


Fig. 1. Stability limits calculated according to (29) (dashed line) and (31) (solid line) as a function of the average power in the laser for a dispersion coefficient of 8 ps/(nm · km), a modulation frequency of 2 GHz, and a fiber length of 50 m. The optimal operating region, marked in the figure, is obtained when both the conditions $\Delta G - l + \text{Re}\{E_o\} > 0$ and $\Delta G - l + \text{Re}\{E_o + E_1\} < 0$ are met. The dotted line shows the stability condition for the solitary pulse calculated according to (10).

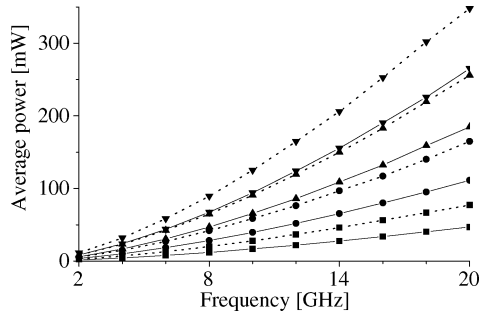


Fig. 2. Boundaries of the average power inside the laser required for optimal operation as a function of the modulation frequency, as calculated according to (29) (solid line) and Eq. (31) (dotted line) for different dispersion coefficients: ■ 2 ps/(nm · km), ● 4 ps/(nm · km), ▲ 6 ps/(nm · km), and ▼ 8 ps/(nm · km).

the solitonic pulse given in (10) (dotted line). The optimal operating region of the laser is marked in the figure. The figure indicates that the minimum power required for stable operation is determined by the requirement that the noise in a time slot where a pulse is dropped will be unstable (31), while the maximum power is determined by the demand that the noise in a time slot where a pulse propagates will be stable (29).

Fig. 2 shows the results of (29) and (31) as a function of the modulation frequency for several values of the dispersion coefficient of the intracavity fiber: 2, 4, 6, and 8 ps/(nm · km).

Fig. 2 shows that the minimum power needed for stable operation of the laser increases as the modulation frequency or the dispersion are increased. The same result is obtained for the upper limit of the power of the optimal operating region. Equations (31) and (32) show that the dependence of the minimum power required to recover from pulse dropout is proportional to $\omega_M^{3/2}$. Using a straightforward complex analysis of the integrals $I[f_M(k, k', \omega_M \tau)]$ and $\bar{I}[f_M(k, k', \omega_M \tau)]$ we have shown that the modulator adds a term to the stability condition that is proportional to $\omega_M^2 \tau^2$. Since the average laser power is $P = W \cdot \omega_M / 2\pi$, where $W = 2D/\tau\delta$ is the pulse energy, (29) indicates that the maximum power is also proportional to $\omega_M^{3/2}$. By fitting the maximum power of the optimal operating region to the function $P = A \cdot \omega_M^n$ we received values of n between 1.475 and 1.498 with errors of 0.021 and 0.010, respectively, in accordance to the expected value of $n = 1.5$. We note that the dependence of the minimum and the maximum average

power needed for stable operation on the modulation frequency is larger than the trivial linear dependence due to the increase in the number of cavity pulses. A similar result was obtained for the stability condition of the soliton in [23]. Since both the lower and the upper power limits depend on the modulation frequency as $\omega_M^{3/2}$, the stable operating regime becomes wider as the modulation frequency increases, as can be seen in Fig. 2.

V. COMPARISON TO A NUMERICAL SIMULATION

In order to validate the use of the variational approach, the reduced model, and the perturbation theory, we analyzed the laser using a comprehensive numerical simulation, similar to that used in [10]. We simulated the pulse propagation in the fiber by solving the scalar nonlinear Schrödinger equation using the split-step Fourier method. We used a model for the Er-doped fiber amplifier that contained the saturation effect of the amplifier as well as the amplified spontaneous emission noise [24]. The number of pulses that simultaneously propagate in the laser cavity is large. For example, in a cavity with a length of 50 m and a modulation frequency of 10 GHz, about 2500 pulses simultaneously propagate in the cavity. Due to the very slow response time of the Er-doped amplifier, all the pulses affect the amplifier saturation. Therefore, we used the super-pulse method [10] to take into account the interaction of the pulses due to the amplifier. This effect is not taken into account in the reduced model. We have simulated the propagation of six pulses. The third pulse was the pulse that was dropped. For each point we simulated the propagation of the pulses through more than 300 000 round-trips in the cavity. The parameters of the laser that was simulated were the same as the parameters that were used in the reduced model described in Section IV.

Fig. 3 demonstrates how the comparison between the results of the reduced model and the results of the numerical simulation was performed. The results shown in the figure correspond to a laser with a modulation frequency of 2 GHz and a dispersion coefficient of 8 ps/(nm·km). The dashed and the solid lines are the results of (29) and (31), in the reduced model, respectively. Points A–D, marked in the figure, were used in the numerical simulation to determine the minimum and the maximum laser power needed for an optimal operation. Fig. 4 shows the pulse train, calculated using the numerical simulation, that corresponds to the four points (A–D) marked in Fig. 3. Fig. 4(a) shows that at the average power that corresponds to point A, the third pulse in the pulse train does not recover from dropout. Fig. 4(b)–(c) gives the pulse train at the boundaries of the optimal operating region. In this region, the third pulse regenerated and the laser could recover from pulse dropout. When the power is further increased, multiple pulses are generated due to the instability of the noise surround the pulses, as shown in Fig. 4(d).

We compared the results of the numerical simulation to the results obtained from (29) and (31) at two different modulation frequencies (2 and 20 GHz) and two dispersion coefficients (2 and 8 ps/nm·km). The four points that were used in the comparison correspond to the extreme points of the boundary of the operating region that were analyzed in Section IV. Assuming that the stability region changes continuously and monotonously as a function of the modulation frequency and the dispersion, as

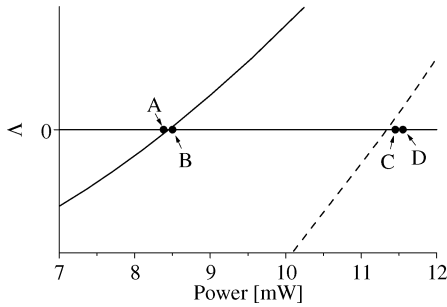


Fig. 3. Comparison between the boundaries of the optimal operating region calculated using the reduced model (solid and dashed lines) and the numerical simulation (points A–D). The boundaries obtained using the reduced model were calculated using (29) (dashed line) and (31) (solid line) as a function of the average power in a laser with a dispersion coefficient of 8 ps/(nm · km) and a modulation frequency of 2 GHz. The stability condition is obtained when both conditions $\Delta G - l + \text{Re}\{E_o\} > 0$ and $\Delta G - l + \text{Re}\{E_o + E_1\} < 0$ are met. Points A–D mark the power of the laser used to determine the boundary of the stable operating region using the numerical simulation.

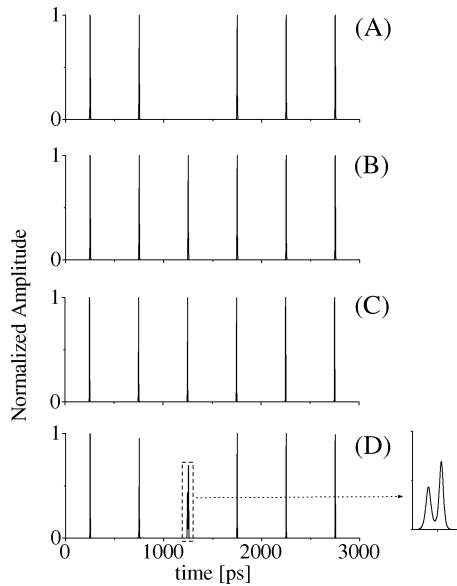


Fig. 4. Pulse train in the four points, marked A–D in Fig. 3, calculated using the numerical simulation. Points B and C give the boundary of the optimal laser operating region where the laser can recover from pulse dropout. In Fig. 4(a) the laser cannot recover from pulse dropout, while in Fig. 4(d), multiple pulses are generated. The results are obtained after simulating the propagation of the pulses along more than 300 000 round-trips.

obtained by the reduced model, the comparison at the boundary points gives an estimate of the difference between the numerical and the reduced model along the whole operating region, analyzed in Section IV. For a repetition rate of 2 GHz (20 GHz) the error between the numerical model and (29) of the reduced model was equal to 3% (12%) and 10% (14%) for a dispersion coefficient of 2 and 8 ps/(nm · km), respectively. The error between the numerical model and (31) for a repetition rate of 2 GHz (20 GHz) was equal to 4% (0%) and 0% (2%) for a dispersion coefficient of 2 and 8 ps/(nm · km), respectively. Therefore, the results of the reduced model are in good quantitative agreement with the results of the comprehensive numerical simulation for the simple laser configuration analyzed. The agreement to which the results of the numerical and the reduced model agree also depends on the number of round-trips

that were simulated. In points B and C of Fig. 4, the gain of the noise is very small, and there is a need to significantly increase the simulation runtime.

The comparison of the reduced model and the numerical simulation gives the overall error in the reduced model, due to the assumptions that led to the master equation, the first order perturbation analysis, and the use of the variational approach. However, the comparison does not separate between the contributions of the individual errors and the contribution of the overall error. The validity of the perturbation theory is studied theoretically in [25]. The validity of the master equation and the perturbation theory was also studied in previous works by comparing the theoretical results to experimental and numerical results [7], [8], [26], [27]. Our numerical results show that when the pulse significantly changes during a round-trip, a large error is obtained in the reduced model. For example, as the filter bandwidth becomes narrower the total error increases also. For a filter with a bandwidth of 3.5 nm (instead of 14 nm used in this manuscript), the total error becomes 21% at a dispersion of 2 ps/(nm · km) and a modulation frequency of 2 GHz, and 62% at a dispersion of 2 ps/(nm · km) and a modulation frequency of 20 GHz, compared to 3% and 12% obtained in the laser analyzed in the previous section. When the dispersion length decreases, the change in the pulse during a round-trip increases and the error becomes larger. The parameters used in our numerical simulation ensure a small change of the pulse along the cavity. The maximum loss of the pulse due to the modulator and the filter, obtained by the numerical simulation close to the upper boundary of the stable operating region, were $3 \cdot 10^{-3}$ and $9 \cdot 10^{-3}$, respectively, when the repetition rate was 20 GHz and the dispersion was 2 ps/(nm · km). We found that the pulse in the numerical simulation had indeed a secant-hyperbolic profile with a correlation to a secant-hyperbolic function better than 0.993. The noise energy was very small, less than 1% of the soliton energy even when the laser power was very close to the boundary of the stable operating region. For example, at a modulation frequency of 20 GHz, a dispersion value of 8 ps/(nm · km), and a laser power of 99.5% of the power at the boundary of the optimal operating region, the noise energy was only 0.5% of the soliton energy. This result indicates that the noise can be accurately calculated, close to the boundary of the stable operating region, using perturbation theory. Moreover, it indicates that the stability of the solution in (21) can be determined by the homogenous part of the equation. Neglecting the higher order terms in (15) can be justified since the maximum of the parameter $\omega_M^4 \tau^4$, is equal to $2.5 \cdot 10^{-4}$ while the lower order parameter $\omega_M^2 \tau^2$ is equal to $1.6 \cdot 10^{-2}$, obtained for a repetition rate of 20 GHz and a pulse duration of 1 ps. The value of the parameter $1/(\Omega_F^2 \tau^2)$ is smaller than $3.5 \cdot 10^{-2}$, obtained for a pulse duration of 1 ps.

VI. CONCLUSION

We have studied theoretically the recovery of a harmonically actively mode-locked soliton fiber laser from pulse dropout. In order to obtain stable operation in practical lasers, pulses that are dropped due to changes in environmental conditions should recover, while other pulses that propagate in the cavity should

remain stable. Soliton perturbation theory was used to find stability conditions for the noise in a time slot where a steady state pulse propagates and in a time slot where a pulse is dropped. In the optimal operating region of the laser, the noise should be stable in the presence of a pulse, while the noise should become unstable in a time slot where a pulse is dropped. This requirement ensures that the laser will recover from accidental pulse dropout. The stabilization of the noise due to the presence of the pulse is caused by the transfer of energy from the continuum accompanying the pulse to the bound states of the solitary pulse by the modulator and the filter. Since solitonic propagation of pulses inside the cavity is stable, noise transferred into the bound states of the solitonic pulses decays. Therefore, the loss of the noise due to the presence of the pulses increases. We found that higher dispersion and higher modulation frequency of the laser stabilize the noise and enable an optimal operation at broader power regions and at shorter pulse durations. A good agreement between the results of the reduced model and the results of a comprehensive numerical simulation was obtained. The result of this paper enable to better understand the causes and to improve the stability of actively mode-locked fiber lasers.

REFERENCES

- [1] J. P. Gordon and H. A. Haus, "Random walk of coherently amplified solitons in optical fiber transmission," *Opt. Lett.*, vol. 11, no. 10, pp. 665–667, 1986.
- [2] H. A. Haus, "A theory of forced mode locking," *IEEE J. Quantum Electron.*, vol. QE-11, no. 7, pp. 323–330, Jul. 1975.
- [3] O. E. Martinez, R. L. Fork, and J. P. Gordon, "Theory of passively mode-locked lasers for the case of a nonlinear complex-propagation coefficient," *J. Opt. Soc. Amer. B*, vol. 2, no. 5, pp. 753–760, 1985.
- [4] H. A. Haus, W. S. Wong, and F. I. Khatri, "Continuum generation by perturbation of soliton," *J. Opt. Soc. Amer. B*, vol. 14, no. 2, pp. 304–313, 1997.
- [5] J. P. Gordon, "Dispersive perturbations of solitons of the nonlinear Schrödinger equation," *J. Opt. Soc. Amer. B*, vol. 9, no. 1, pp. 91–97, 1992.
- [6] H. A. Haus and A. Mecozzi, "Noise of mode-locked lasers," *IEEE J. Quantum Electron.*, vol. 29, no. 3, pp. 983–995, Mar. 1993.
- [7] D. J. Kaup, "Perturbation theory for solitons in optical fibers," *Phys. Rev. A*, vol. 42, no. 9, pp. 5689–5694, 1990.
- [8] F. X. Kaertner, D. Kopf, and U. Keller, "Solitary-pulse stabilization and shortening in actively mode-locked lasers," *Phys. Rev. A*, vol. 12, no. 3, pp. 486–496, 1995.
- [9] S. Namiki and H. Haus, "Noise of the stretched pulse fiber laser: part I—theory," *IEEE J. Quantum Electron.*, vol. 33, no. 5, pp. 660–668, May 1997.
- [10] M. Horowitz, C. R. Menyuk, T. F. Carruthers, and I. N. Duling III, "Theoretical and experimental study of harmonically modelocked fiber lasers for optical communication systems," *J. Lightw. Technol.*, vol. 18, no. 11, pp. 1565–1574, Nov. 2000.
- [11] D. J. Kuizenga and A. E. Siegman, "FM and AM mode locking of the homogeneous laser—part I: theory," *IEEE J. Quantum Electron.*, vol. QE-6, no. 11, pp. 694–708, Nov. 1970.
- [12] A. Takada and H. Miyazawa, "30 GHz picosecond pulse generation from actively mode-locked erbium-doped fiber laser," *Electron. Lett.*, vol. 26, no. 3, pp. 216–217, 1990.
- [13] A. D. Ellis, R. J. Manning, I. D. Phillips, and D. Nasset, "1.6 ps pulse generation at 40 GHz in phaselocked ring laser incorporating highly nonlinear fiber for application to 160 Gbit/s OTDM networks," *Electron. Lett.*, vol. 35, no. 8, pp. 645–646, 1999.
- [14] H. Haus and A. Mecozzi, "Long term storage of a bit stream of solitons," *Opt. Lett.*, vol. 17, no. 21, pp. 1500–1502, 1992.
- [15] M. E. Grain, H. A. Haus, Y. Chen, and E. P. Ippen, "Quantum-limited timing jitter in actively modelocked lasers," *IEEE J. Quantum Electron.*, vol. 40, no. 10, pp. 1458–1470, Oct. 2004.
- [16] W. Kaplan, *Ordinary Differential Equations*. Reading, MA: Addison-Wesley, 1958.
- [17] M. S. Miguel and R. Toral, *Instabilities and Non-Equilibrium Structures, IV*, E. Tirapegui, J. Martinez, and R. Tiemann, Eds. Norwell, MA: Kluwer, 2000.
- [18] A. Jannussis, G. Brodimas, S. Baskoutas, and A. Leodaris, "Non-hermitian harmonic oscillator with discrete complex or real spectrum for nonunitary squeeze operators," *J. Phys. A: Math. Gen.*, vol. 36, pp. 2507–2516, 2003.
- [19] A. Kostenbauder, Y. Sun, and A. E. Siegman, "Eigenmode expansions using biorthogonal functions: complex-valued hermite-gaussians," *J. Opt. Soc. Amer. A*, vol. 14, no. 8, pp. 1780–1790, 1997.
- [20] C. H. Chen and C.-D. Lien, "The variational principle for nonself-adjoint electromagnetic problems," *IEEE Trans. Microw. Theory Tech.*, vol. MTT-28, no. 8, pp. 878–886, Aug. 1980.
- [21] C. Cohen-Tannoudji, B. Diu, and F. Laloe, *Quantum Mechanics*. New York: Wiley, 1977.
- [22] T. F. Carruthers and I. N. Duling III, "10-GHz, 1.3-ps erbium fiber laser employing soliton pulse shortening," *Opt. Lett.*, vol. 21, no. 23, pp. 1927–1929, 1996.
- [23] M. Horowitz and C. R. Menyuk, "Analysis of pulse dropout in harmonically mode-locked fiber lasers by use of the Lyapunov methods," *Opt. Lett.*, vol. 25, no. 1, pp. 40–42, 2000.
- [24] M. Horowitz, C. R. Menyuk, and S. Keren, "Modeling the saturation induced by broad-band pulses amplified in an erbium-doped fiber amplifier," *IEEE Photon. Technol. Lett.*, vol. 11, no. 10, pp. 1235–1237, Oct. 1999.
- [25] T. Georges, "Perturbation theory for the assessment of soliton transmission control," *Opt. Fib. Technol.*, vol. 1, no. 2, pp. 97–116, 1994.
- [26] D. J. Jones, H. A. Haus, and E. P. Ippen, "Subpicosecond solitons in an actively mode-locked fiber laser," *Opt. Lett.*, vol. 21, no. 22, pp. 1818–1820, 1996.
- [27] M. E. Grein, L. A. Jiang, Y. Chen, H. A. Haus, and E. P. Ippen, "Timing restoration in an actively mode-locked fiber ring laser," *Opt. Lett.*, vol. 24, no. 23, pp. 1687–1689, 1999.

Avi Zeitouny was born in Haifa, Israel, in 1971. He received the B.A. degree in physics in 1996, the B.Sc. degree in materials engineering in 1996, and the M.Sc. degree in materials engineering in 1999, from the Technion-Israel Institute of Technology, Haifa, Israel. He is currently working toward the Ph.D. degree in electrical engineering at the Technion.

His research interests include fiber lasers and their applications.

Yuriy N. Parkhomenko was born in Kyiv, Ukraine, in 1945. He graduated Kyiv State National University, Kyiv, Ukraine, in 1974. He received the Ph.D. degree in physics and mathematics in 1981, and the Dr.Sc. degree in physics and mathematics (optics, laser physics) in 1996 from Kyiv National University in 1996.

He joined the Institute of Physics of National Academy of Sciences of Ukraine (NASU), in 1984, where he was Senior Research Fellow, and the Institute of Applied Problems of Physics and Biophysics of NASU (Kyiv, Ukraine) in 1991, where he was Head of Laboratory of Laser Physics and Spectroscopy. He was engaged in research in the problem of tunable lasers, optical diffraction, and quantum electronics. In 2003, he joined the Technion-Israel Institute of Technology, Haifa, Israel, where he is working in the field of laser physics and diffraction theory. He is the author and coauthor of over 100 papers.

Moshe Horowitz received the Ph.D. degree from the Technion-Israel Institute of Technology, Haifa, Israel, in 1994.

Since 1998, he has been a Professor with the Department of Electrical Engineering, Technion. His current research interests include inverse scattering theory in fiber gratings and its applications for developing novel fiber sensors, novel fiber lasers, and microwave photonics.